Available online www.jsaer.com

***Journal of Scientific and Engineering Research*, 2021, 8(9):76-82**

Research Article

ISSN: 2394-2630
CODEN(USA): JSERBR

Adjustable Magnetic Anisotropy of Patterned Electroless Co-Ni-P Film by Laser Etching

Jing Yuan

College of Physics Electronic Information Engineering, Qinghai Minzu University, Xining, Qinghai 810007, P R China

Abstract Co-Ni-P soft magnetic coating with the coercivity of 4Oewas electroless plated onto silicon wafer substrate. The surface morphology, thickness, composition and magnetic properties of the plating were observed and determined by scanning electron microscope (SEM), energy dispersive X-ray spectrometry (EDX), X-ray diffractometer (XRD) and vibrating sample magnetometer (VSM).Co-Ni-P plating after laser etching displayed the in-plane uniaxial anisotropy related to the stripe width, and the in-plane anisotropy decreased as the stripe width increased. When the width of Co-Ni-P stripe increased from 0.06mm to 0.25mm, the in-plane anisotropy decreased from 301Oe to 95Oe. In addition, the coercivity of the etched Co-Ni-P plating have been significantly increased compared with the as-prepared plating, which might be due to the phase change or internal stress of the coating caused by laser etching has an impact on the magnetic properties of the film.

Keywords electroless Co-Ni-P plating, laser etching, magnetic anisotropy

1. Introduction

Electroless Co-Ni-P ternary alloy deposits possesses a characteristic in magnetism, such as low coercivity and high saturation magnetization, so it is generally considered as a soft magnetic material [1, 2]. The film thickness, chemical composition, crystal structure and microstructure can determine the magnetic properties of Co-Ni-P film, and these factors can be controlled by adjusting the plating bath composition and the operation parameters [3,4]. Dong-Hyun et al. prepared electroless Co-Ni-P ternary alloy deposits with soft magnetic characteristics on copper sheet substrate, and found the saturation magnetization, remanence and coercivity of Co-Ni-P film are increased with cobalt content of the deposit [5]. Narayanan et al. studied the effect of $CoSO_4/(NiSO_4 + CoSO_4)$wt.% in plating bath on the plating rate, composition and crystallinity, and the results showed that when the $NiSO_4/(NiSO_4 + CoSO_4)$ wt.% in plating bath is 10, the Ni/(Co + Ni + P) wt.% in film is above 30 and the plating rate of electroless film is greatly increased [6]. Considering the magnetic properties and plating speed comprehensively, when the ratio of Ni^{2+} concentration to Co^{2+} concentration in the plating solution is 2:4, the film prepared with excellent soft magnetic properties and suitable plating speed.

An in-plane uniaxial magnetic anisotropy is required when the soft magnetic films are used in various applications such as magnetic recording heads and microwave noise filters. There are several methods to obtain the in-plane uniaxial magnetic anisotropy including applying an inducing magnetic field during deposition, magnetic field annealing and oblique sputtering, etc [7-9]. Film patterning with periodic structure is a feasible way to induce the in-plane magnetic anisotropy, and obtain the required anisotropy field by controlling the stripe width [10]. However, the demagnetization effect is evident when the strip widths are in nanometer order, but there are few literatures on the adjustment the in-plane magnetic anisotropy filed when the strip widths are in micrometer order.

In this article, Co-Ni-P alloy coating was successfully deposited on surface of silicon wafer by electroless plating technology. There are two laser etching methods are used to obtain in-plane uniaxial anisotropy on the surface of Co-Ni-P plating. Co-Ni-P plating after laser etching displayed the in-plane uniaxial anisotropy related to the stripe width, and the in-plane anisotropy decreased as the stripe width increased.

2. Materials and Methods

2.1. Preparation

Co-Ni-P film was prepared on silicon wafer by electroless plating method. Before plating, silicon substrate was treated by cleaning, dipping, sensitizing and activation processes sequentially which described in reference [11]. After the pretreatment, the silicon substrate was immediately put into the electroless plating bath for the preparation of Co-Ni-P coating. The bath composition and other parameters were given in Table 1. The specimen were coated for 10min, removed from the bath, washed with water and dried with electric drier.

Table 1: Composition of the electroless plating bath and operating conditions

Bath constituents and parameters	Operating conditions
$Ni_2SO_4 \cdot 6H_2O$ 0.024 mol/L	
$CoSO_4 \cdot 6H_2O$0.036 mol/L	Temperature = 85℃
$NaH_2PO_2 \cdot H_2O$ 0.1 mol/L	pH=9.0
$Na_3C_6H_5O_7 \cdot 2H_2O$40g/L	Mild-mechanical agitation
$(NH_4)_2SO_4$40g/L	

In this experiment, laser etching was used to obtain the strip arrays pattern, and the laser etching diagram was shown in Figure 1. The strip orientations was along any direction of the silicon surface. The widths of magnetic strip (x) were varied from 0.06 to 0.25 mm and the separation gap between strips is 0.02mm. Two types of laser patterned samples were prepared. One type of samples were to perform laser etching on the silicon substrate first, and then electroless plated on the surface of the etched substrate. Another sample was to electroless plating on silicon substrate first, and then performed laser etching.

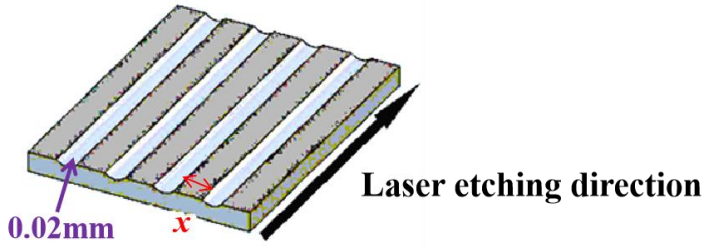

Figure 1: Schematic diagram of laser etching

2.2. Characterization

The surface and cross section morphology of Co-Ni-P coating were observed by electron microscopy (FESEM, Hitachi S-4800, Japan) operated at 5.0 kV, and the composition of plating was determined by the energy-dispersive X-ray spectrometry (EDS). And the thickness of the plating was directly measured from the cross-section images. The magnetic properties of Co-Ni-P coating was determined by using vibrating sample magnetometer (VSM, Lakeshore 7304, America) at room temperature.

3. Results & Discussion

3.1. The Morphology and Composition of Co-Ni-P Plating

Figure 2 is the surface and cross-section morphology, the composition and the magnetic hysteresis curve of the electroless Co-Ni-P plating. The Co-Ni-P plating consists of a large number of nodular structure, and the structure size is between a few microns and a dozen microns. The average thickness of the Co-Ni-P plating has reaches 760 nm. The plating is mainly composed of Ni, Co and P, and the contents of these three elements is shown in Table 2. The concentration ratio of Ni^{2+} and Co^{2+} in the plating solution is 2:4, but the content ratio of these three elements in the coating is about 37.3 ± 0.8: 55.5 ± 1.1. This result reflected that the deposition rate of the two metallic elements are significantly different. Compared with Co, metallic Ni is easier to deposit.

Because the reduction potential of Ni^{2+} and Co^{2+} are −0.22 eV and −0.28 eV , the rate (v) of reduction and deposition is $v_{Ni^{2+}} > v_{Co^{2+}}$ [12]. The Co-Ni-P plating as prepared has excellent soft magnetic properties, and the coercivity of the plating is only 4Oe.

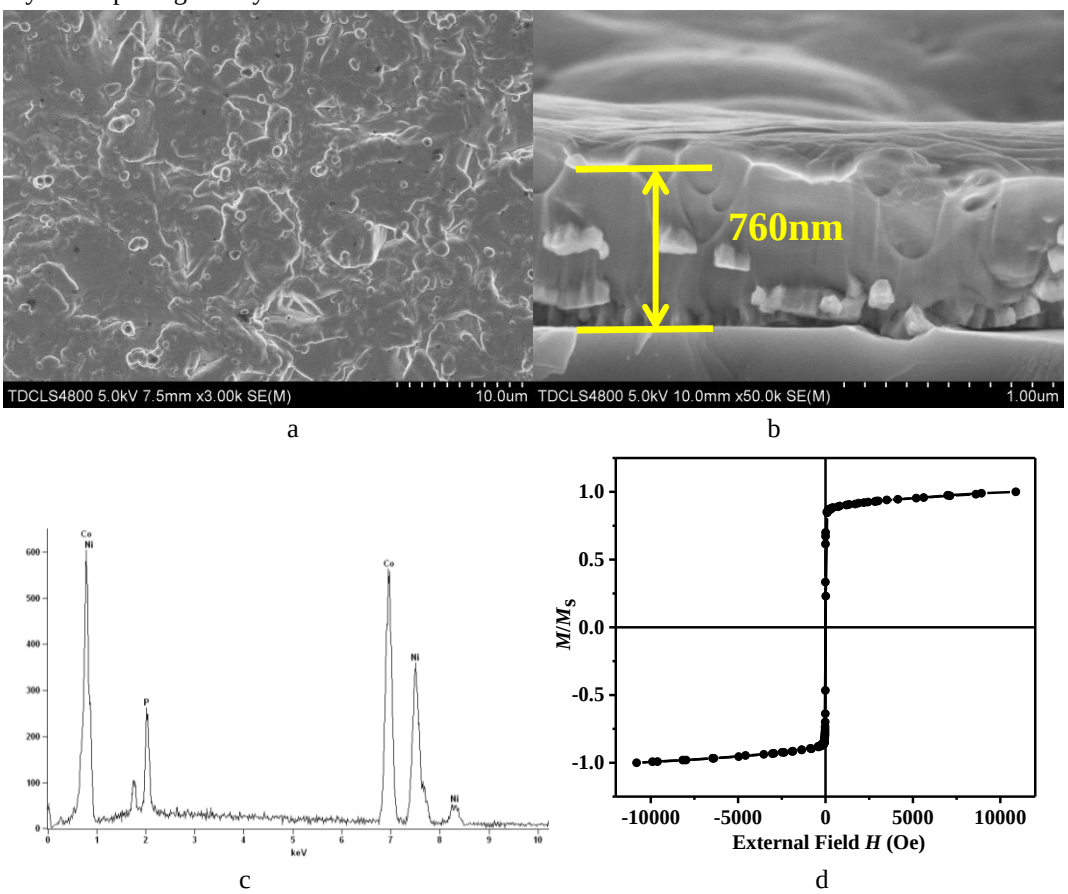

Figure 2: The morphologies and composition of Co-Ni-P plating, (a) the surface morphology, (b) the cross-section view, (c) the composition and (d) magnetic hysteresis curve.

Table 2: Elementary composition of Co-Ni-P plating

Elements	Weigh content (%)	Weight error (%)	Atom content (%)	Atom error (%)
P	7.2	± 0.3	12.8	± 0.6
Co	55.5	± 1.1	52.0	± 1.0
Ni	37.5	± 0.8	35.2	± 0.7

3.2. Electroless Co-Ni-P plating on the silicon substrate after laser etching

Figure 3 shows the optical images and magnetic hysteresis curves of Co-Ni-P plating prepared on the etched silicon substrate. The widths of stripe (x) on silicon substrate are 0.06mm, 012mm and 0.17mm. It can be seen from that the hysteresis loop of the laser etching along the etching direction and the vertical etching direction has been significantly different. The magnetic moment along the etching direction is easy to magnetize, while the magnetic moment perpendicular to the etching direction is difficult to magnetize, and an in-plane anisotropy field appears. But the in-plane anisotropy field doesn't change with the spacing of the magnetic stripes. When the widths of magnetic strip is 0.06mm, 0.12mm and 0.17mm respectively, the in-plane anisotropy field is 30Oe, 70Oe and 0Oe. Although the in-plane anisotropy field can be obtained by this method, the in-plane anisotropy field does not change regularly with the width of the magnetic stripe, the idea of controlling the in-plane anisotropy field by adjusting the stripe width is not easy to achieve. Therefore, in the next experiment,

(b)

electroless Co-Ni-P plating is applied on the surface of silicon substrate, and then the plating layer is laser etched.

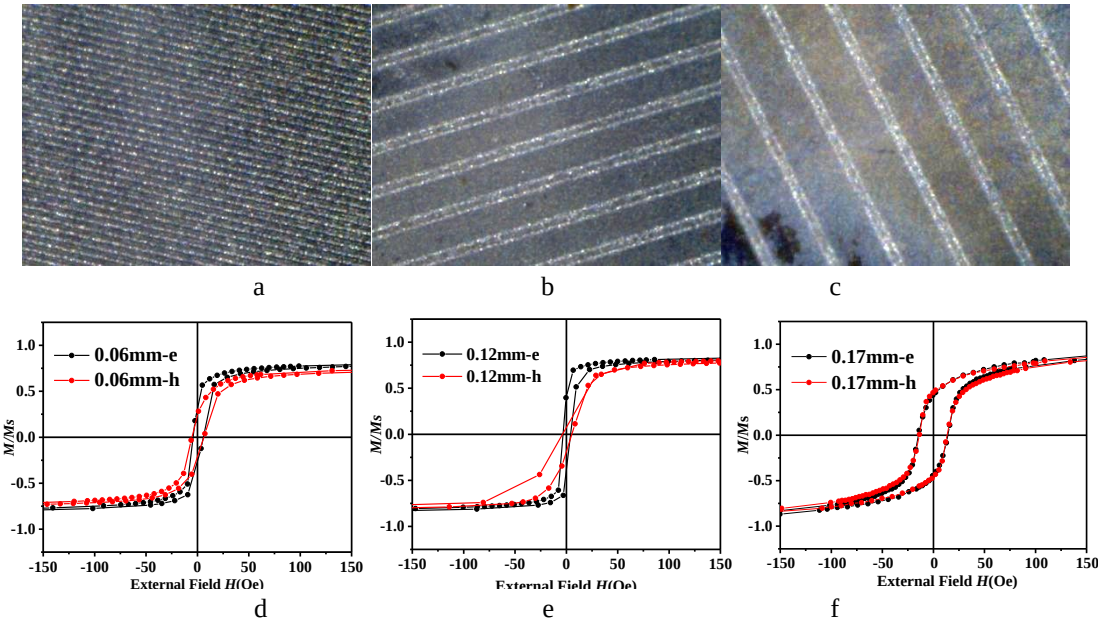

Figure 3: Optical microscope images and magnetic hysteresis curves of Co-Ni-P plating prepared on the surface of silicon substrate etched with different line widths, (a) and (d) 0.06mm, (b) and (e) 0.12mm, (c) and (f) 0.17mm.

3.3. Laser etching after electroless Co-Ni-P plating on silicon substrate

Figure 4 shows the optical images and magnetic hysteresis curves of the laser etched Co-Ni-P plating. The widths of Co-Ni-P stripe (x) changed from 0.06mm to 0.25mm, and the Co-Ni-P stripes presents a series of regular in-plane anisotropic fields along the etching direction and the vertical etching direction. And the anisotropy field changes linearly with the width of the Co-Ni-P stripe.

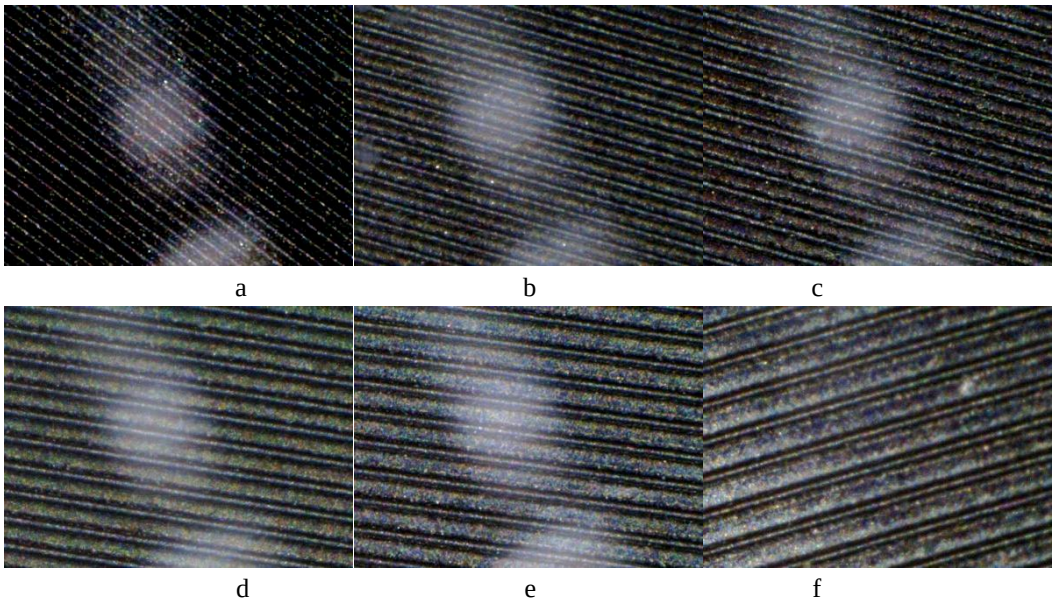

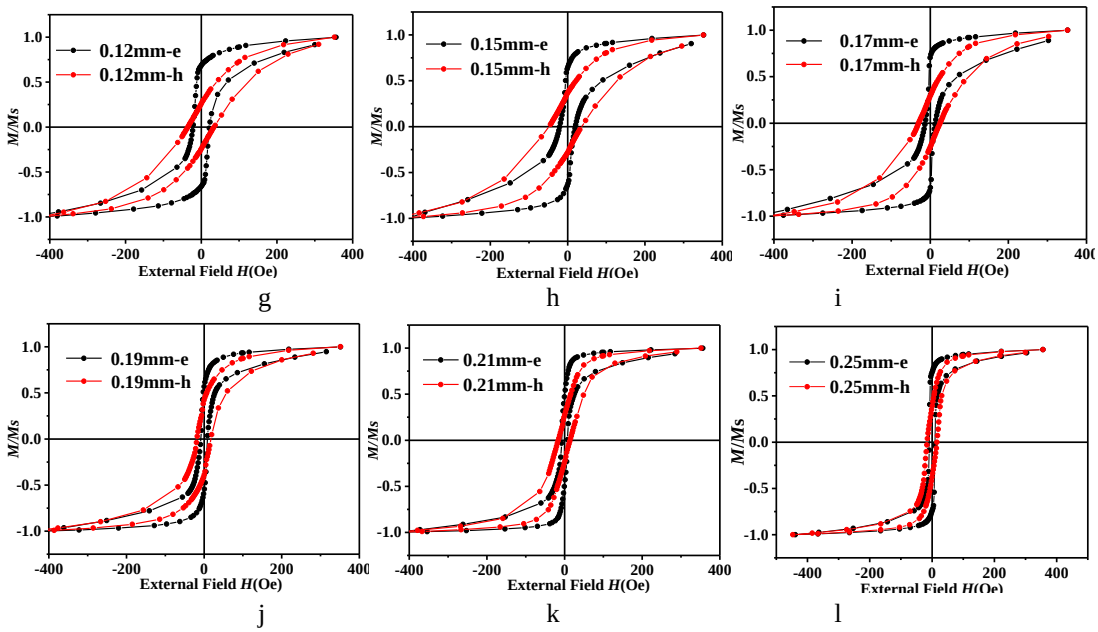

Figure 4: Optical microscope images and magnetic hysteresis curves of Co-Ni-P plating after etched with different line widths, (a) and (g) 0.12mm, (b) and (h) 0.15mm, (c) and (i) 0.17mm, (d) and (j) 0.19mm, (e) and (h) 0.21mm, (f) and (l) 0.25mm.

Figure 5 is the relationship between the width of the Co-Ni-P stripe and in-plane anisotropy filed. In general, the Co-Ni-P stripe with a smaller line width corresponds to a larger anisotropy field, and the Co-Ni-P stripe with a larger line width corresponds to a smaller anisotropy field. When the stripe width increases from 0.06mm to 0.25mm, the in-plane anisotropy field decreases from 301Oe to 95Oe. Because the width of the stripe is in the micron level, and the magnetic domain size of the soft magnetic material is also in the micron or sub-micron level, the laser etching induces the in-plane magnetic anisotropy. The anisotropy field can be controlled by the width of Co-Ni-P stripe.

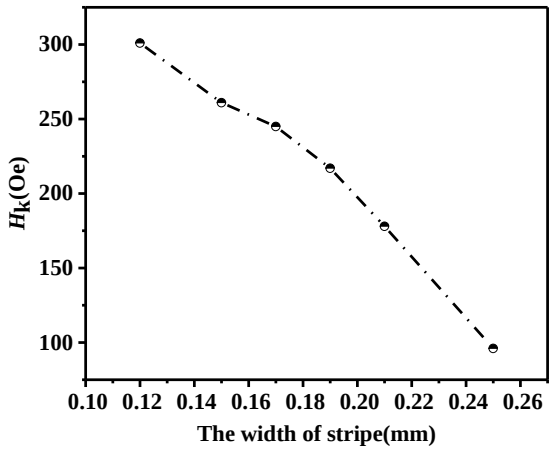

Figure 5: The relationship between the stripe width and the in-plane anisotropy field

Figure 6 shows the relationship between Co-Ni-P stripe width and coercivity of easy and hard magnetization axis. The coercivity of the etched Co-Ni-P plating have been significantly increased compared with the as-prepared Co-Ni-P plating, and there is an obvious bee waist in the hysteresis loop in the direction of the easy magnetization axis. This may be due to the rapid heating of the part of the film caused by laser etching to produce a phase change, and the stress caused by the etching process also has an impact on the magnetic properties of the film. The coercivity basically shows a downward trend as the width of stripe increases. When the width of stripe is small, the area of the film that is etched by the laser is larger, the area of the film that is

etched by the laser is larger, and local rapid heating may crystallize the film, so the coercive force of the film increases. As the width of stripe becomes large, the area of the film that is etched by the laser changes small, the area of the rapidly heated film becomes smaller, and most of the film maintains the original structure, so the coercivity of the striped structure at this time is closer to the coercivity of the untreated film.

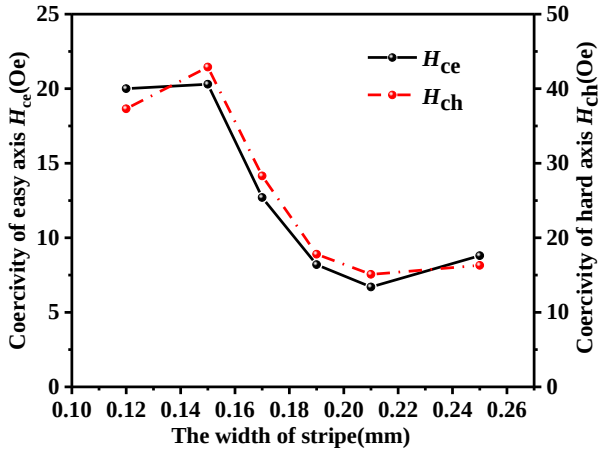

Figure 6: The relationship between the stripe width and coercivity of easy and hard magnetization axis

4. Conclusion

There were two strategies used to obtain in-plane uniaxial anisotropy on the surface of elctroless Co-Ni-P plating, and the results obtained were as follows:

(1) Co-Ni-P plating prepared on the etched silicon substrate showed an in-plane uniaxial anisotropy along the etched direction and the vertical etching direction, but the in-plane uniaxial anisotropy didn't related to the stripe width on silicon substrate, it was difficult to control the anisotropy field by controlling the stripe width.

(2) Co-Ni-P plating after laser etching displayed the in-plane uniaxial anisotropy related to the stripe width on Co-Ni-P surface, and the in-plane anisotropy decreased as the stripe width increased. When the width of Co-Ni-P stripe increased from 0.06mm to 0.25mm, the in-plane anisotropy field decreased from 301Oe to 95Oe. In short, this strategy provided a way that can achieve large-scale control of the in-plane anisotropy field of the magnetic film.

References

[1]. Siyi, B., Hang, Z., Lei, H., & Yinxiang, Lu. (2017). Comparative study of electroless Co-Ni-P plating on Tencel fabric by Co0-based and Ni0-based activation for electromagnetic interference shielding. *Applied Surface Science, 419*, 465-475.

[2]. Fangxu, N., Yanxiang, W., Lianru, M., Ziyi, X., Yaoyao, W., Chengguo, W., & Yanpeng, M. (2019). Achieving enhanced dielectric property via growing Co-Ni-P nano-alloys on SiC nanowires with 3D conductive network. *Journal of Alloys and Compounds, 778*, 933-941.

[3]. H. Matsuda, H., Jones, G.A., Takano, O., & Grundy, P.J. (1993). Room-temperature electroless deposition of high-coercivity Co-Ni-P films. *The Journal of Magnetism and Magnetic Materials, 120*, 338-341.

[4]. Katya I., Momchil A., Stephan K., Yordanka M., Stela V., & Georgi A. (2019). Effect of H3PO4 and NaH_2PO_2 in the electrolyte on the composition and microstructure of Ni-Co-P alloys. *Journal of chemical technology and metallurgy, 54* (6), 1271-1280.

[5]. Dong-Hyun, K., Koji, A., & Osamu, Takano. (1999). Soft magnetic films by electroless Ni-Co-P plating. *Journal of Electrochemical Society, 142* (11), 3763-3767.

[6]. Narayanan, T., S. Selvakumar., & Stephenb, A. (2003). Electroless Ni-Co-P ternary alloy deposits: preparation and characteristics. *Surface and Coatings Technology, 172* (2-3), 298-307.

[7]. Nguyenduy, H., Manh-huong, P., & Chong Oh, K. (2007). Novel nanostructure and magnetic properties of Co-Fe-Hf-O films. *Nanotechnology, 18* (15), 155705.

[8]. Cuiling W., Shouheng Z., Shizhu Q., Honglei D., Xiaomin L., Ruicong S., Xianming C., Guoxing M., Youyong D., Shishou K., Shishen Y., & Shandong, L. (2018). Dual-mode ferromagnetic resonance in an FeCoB/Ru/FeCoB synthetic antiferromagnet with uniaxial anisotropy. *Applied Physics Letters, 112*, 192401.

[9]. Yu, E., Jongsik, S., Inyoung, K., Jongryoul, K., Sukhee, H., Hijung, K., Kihyeon K., & Yamaguchi, M. (2005). Development of FeCo-based thin films for gigahertz applications. *IEEE Transactions on Magnetics, 41* (10), 3259-3261.

[10]. Zhenkun W., Erxi F., Weiwei W., Zhi M., Qingfang L., Jianbo W., & Desheng X. (2012). Adjustable magnetic anisotropy and resonance frequency of patterned ferromagnetic films by laser etching. *Journal of Alloys and Compounds, 543*, 197-199.

[11]. Jing Y., Jihui W., Yun G., Jing M., & Wenbin H. (2017). Preparation and magnetic properties of Ni-Co-P-Ce coating by electroless plating on silicon substrate. *Thin Solid Films, 632*, 1-9.

[12]. Yu, W., Wei, W., Xiaodong, Dan, Y. (2020). Multilayer-structured Ni-Co-Fe-P/polyaniline/polyimide composite fabric for robust electromagnetic shielding with low reflection characteristic, *Chemical Engineering Journal, 380*, 122553.